This article has been accepted for inclusion in a future issue of this journal. Content is final as presented, with the exception of pagination.

Distributed Power Profile Tracking for Heterogeneous Charging of Electric Vehicles

Akshay Malhotra, Giulio Binetti, *Member, IEEE*, Ali Davoudi, *Senior Member, IEEE*, and Ioannis D. Schizas, *Member, IEEE*

***Abstract*—Coordinated charging of plug-in electric vehicles (PEVs) can effectively mitigate the negative effects imposed on the power distribution grid by uncoordinated charging. Simultaneously, coordinated charging algorithms can accommodate the PEV user's needs in terms of desired state-of-charge and charging time. In this paper, the problem of tracking an arbitrary power profile by coordinated charging of PEVs is formulated as a discrete scheduling process, while accounting for the heterogeneity in charging rates and restricting the charging to only the maximum rated power. Then, a novel distributed algorithm is proposed to coordinate the PEV charging and eliminate the need for a central aggregator. It is guaranteed to track, and not exceed, the power profile imposed by the utility, while maximizing the user convenience. A formal optimality analysis is provided to show that the algorithm is asymptotically optimal in case of Homogeneous charging, while it has a very small optimality gap for the heterogeneous case. Numerical simulations considering realistic charging scenarios with different penetration levels and tracking of a valley-filing profile are presented to validate the proposed charging algorithm.**

***Index Terms*—Coordinated charging, distributed algorithm, power profile tracking, plug-in electric vehicle.**

I. Introduction

PLUG-IN electric vehicles (PEVs) are the building blocks of a transportation electrification paradigm. However, uncoordinated charging of a large fleet can have adverse effects on the power grid, including increased peak load, transmission loss, and stress on distribution transformers [1]–[5]. Coordinated charging strategies can address such negative effects. From the user's perspective, the convenience of charging the battery to a desired state-of-charge (SOC) within the required charging time is important. This user convenience can be quantified as a function of battery capacity and charging time [6], [7]. From the utility perspective, it is important to reduce the peak and variance of the load profile imposed on the grid by PEVs [8]. Moreover, the grid operator may require the PEVs to track a charging profile, e.g., to address the intermittency of renewable energies [9] or exhibit a valley-filling profile [10], [11], in a centralized [12] or decentralized [13] fashion.

Often-neglected practical aspects in coordinated charging of PEVs include the limitation of charger technologies and the heterogeneity of the charging process. Most charging schemes consider a continuous charging scenario, e.g., [7], [10], [14] to name a few, where the PEVs can withdraw any power from the grid. However, in practice PEVs are charged with power electronics chargers with given power ratings. Discrete charging scenarios can be formulated as a scheduling problem at the charger's maximum power rating. The on/off switching behavior of discrete charging process may potentially allow the battery some cool off time and mitigate rapid temperature rise, an important factor for battery lifetime longevity [15]. Very few existing work discuss heterogeneous charging scenarios, e.g., [6], [8], [16]–[20]. In general, heterogeneous coordinated charging of PEVs, with discrete charging rates, is largely unexplored.

Existing decentralized charging strategies distribute the computational overhead from the central aggregator to the PEVs, with a hierarchical, tree-like, communication topology. In [6], a two-layer hierarchical structure is considered, where sub-aggregators (SAs) accumulate data from a set of PEVs and report them to the central aggregator constraining the power at both layers. In [21], a layered structure, with constraints accounting for the entire distribution grid, is considered. The algorithms with a central aggregator need a high level of network connectivity, and require high-bandwidth communication links to exchange data. Moreover, in centralized systems, the central aggregator exposes a single point-of-failure, i.e., the failure of the aggregator results in the collapse of the entire system. Similarly, in a hierarchical setup (e.g., [6] and [21]), if the link between a sub-aggregator and the central aggregator collapses, all the PEVs under the SA will be left uncontrolled. Alternatively, distributed charging scenarios replace the central aggregator with multiple sub-aggregators that communicate amongst themselves. Thus, even if a link between two SAs is broken, an alternative communication path connecting the SAs could be used, and the distributed framework is still functional.

Manuscript received April 27, 2015; revised August 14, 2015 and November 13, 2015; accepted January 4, 2016. This work was supported in part by the National Science Foundation under Grant ECCS-1405173 and Grant CCF-1218079, and in part by the U.S. Office of Naval Research under Grant N00014-14-1-0718. Paper no. TSG-00471-2015.

A. Malhotra, A. Davoudi, and I. D. Schizas are with the Department of Electrical Engineering, University of Texas at Arlington, Arlington, TX 76010 USA (e-mail: akshay.malhotra@mavs.uta.edu; davoudi@uta.edu; schizas@uta.edu).

G. Binetti is with the Department of Electrical and Information Engineering, Polytechnic University of Bari, Bari 70125, Italy (e-mail: giulio.binetti@poliba.it).

Color versions of one or more of the figures in this paper are available online at http://ieeexplore.ieee.org.

Digital Object Identifier 10.1109/TSG.2016.2515616

1949-3053 © 2016 IEEE. Personal use is permitted, but republication/redistribution requires IEEE permission.
See http://www.ieee.org/publications_standards/publications/rights/index.html for more information.

This article has been accepted for inclusion in a future issue of this journal. Content is final as presented, with the exception of pagination.

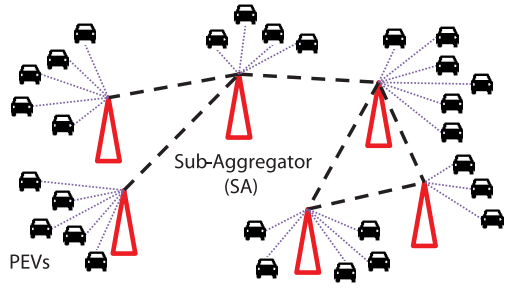

Fig. 1. Example of a sparse communication network with 6 sub-aggregators.

If a SA goes down, of course the PEVs connected to it will remain uncontrolled. Thus, the main advantage of a distributed architecture is that, since there is no central aggregator as in a hierarchical or centralized setting, not all PEVs end up being uncontrolled in the case of a single failure.

The main contributions of the paper are the following:

- The problem of tracking an arbitrary power profile by coordinated charging of PEVs is formalized considering the realistic case of PEVs with different charging rates (*heterogeneous scenario*). Thus, the classical valley-filling behavior is just a sub-case of the more general problem considered in this work.
- A novel distributed algorithm coordinates the PEV charging and eliminates the need for a central aggregator. It is guaranteed to track, and not exceed, the power profile imposed by the power utility, while maximizing the user convenience.
- A formal optimality analysis of the proposed algorithm is provided. Asymptotic optimality is proven in the case of homogeneous charging. An optimality gap is derived for the heterogeneous case and shown to be very small in practical settings (ensuring near optimality).

The rest of this paper is organized as follows. Section II formulates the charging process as a scheduling algorithm and defines a user convenience function based on battery SOC and plug-off time. In Section III, the proposed distributed charging algorithm is discussed and an optimality analysis is provided. In Section IV, the algorithm effectiveness is demonstrated by tracking different target profiles and studying different penetration levels. The complexity and scalability of the algorithm is also discussed. Finally, Section V provides concluding remarks.

II. Problem Formulation

A. Sub-Aggregator Configuration

PEVs are divided amongst disjoint groups, each represented by a SA. The SA is a virtual entity, which communicates only with the PEVs in its respective group and with some of the neighboring SAs in the power distribution network. An example of a charging platform, with six SAs, is shown in Fig. 1. This architecture can be exploited by a distributed algorithm to coordinate PEV charging with a low communication rate between a PEV and its SA, and a higher communication rate among SAs. This cyber architecture can be mapped into the physical power distribution network [6]. The SA can be mapped onto a power substation that receives power from the grid and distributes it locally among PEVs. Thus, since the total available power from the grid is assumed to be limited, a coordination among SAs is required. In addition, a SA can also handle the transformer capacity, i.e., the limit on the maximum power available at a substation.

B. Problem Statement

Assume the charging time horizon is discretized in time slots of a few minutes each (e.g., 15 minutes). For a given time slot, the total number of PEVs to be charged is N, the number of SAs is K, and the number of PEVs in the k-th SA is N_k. For the k-th SA, the set of connected PEVs is denoted by $\mathcal{S}_k$, thus, $N_k = |\mathcal{S}_k|$ (the cardinality of set $\mathcal{S}_k$).

The charging strategy is controlled by binary decision variables via which each PEV is either allowed, or denied to charge during each time slot. The coordinated charging problem is focused on selecting PEVs to charge during each time slot, while fulfilling the power grid constraints and maximizing the user convenience. The problem formulation is motivated by the one discussed in [6] and can be expressed as

$$\text{maximize:} \quad J = \sum_{k=1}^{K} \sum_{i=1}^{N_k} J_{i,k} L_{i,k} s_{i,k} \tag{1}$$

$$\text{subject to} \quad \sum_{i=1}^{N_k} s_{i,k} L_{i,k} \leq P_k \tag{2}$$

$$\sum_{k=1}^{K} \sum_{i=1}^{N_k} s_{i,k} L_{i,k} \leq P \tag{3}$$

where $s_{i,k} \in \{0, 1\}$ denotes the binary charging variable for i-th PEV in k-th SA at the rated power $L_{i,k}$. The objective function J in (1) is the cumulative user convenience function, where $J_{i,k}$ is the user convenience function per unit power for the i-th PEV in the k-th SA. Thus, the user convenience for the i-th PEV in the k-th SA is given by $J_{i,k}L_{i,k}$; more details on the user convenience function per unit power, $J_{i,k}$, are provided in the next section. The constraints (2) and (3) represent the limits on the available power to each SA, P_k, and to all PEVs, P. In details, the constraint (2) relates to the maximum power accessible to the k-th SA which takes into account the physical limitations of the substation. Instead, the constraint (3) states that the total power to charge the PEVs cannot exceed the available power. In line with [22], a successful PEVs charging strategy should conceal the EV penetration from the system to maintain the original peak demand level without PEVs. Thus, to achieve this goal, the maximum available power P is set to the original peak demand level as in [6].

C. User Convenience

The present work proposes the following function to quantify the user convenience per unit power required in (1):

$$J_{i,k} = \frac{SOC_{i,k}^{desired} - SOC_{i,k}^{current}}{L_{i,k} \cdot \max\left(1, t_{i,k}^{plug-off} - t_{curr}\right)} \tag{4}$$

This article has been accepted for inclusion in a future issue of this journal. Content is final as presented, with the exception of pagination.

where $SOC_{i,k}^{desired}$ and $SOC_{i,k}^{current}$ represent the expected SOC at the plug-off time, $t_{i,k}^{plug-off}$, and the SOC at the current time, t_{curr}, respectively, for i-th PEV in k-th SA. This function is inspired from the weights function in [6].

The user convenience value in (4) includes remaining SOC, remaining time to charge, and charging rate. The numerator is the percentage of remaining SOC to fully satisfy the user, considering the desired SOC at the plug-off time. Its range is [0, 100], and it decreases to 0 when the battery is charged (i.e., $SOC_{i,k}^{current} = SOC_{i,k}^{desired}$). The denominator includes the PEV charging rate, $L_{i,k}$, and the remaining time for charging with respect to the expected plug-off time provided by the user at the plug-in time. The charging rate provides a user convenience per unit power. The times are expressed in time slot units, so that in a day they range from 0 to 96, assuming 15 minute time slot each. The maximum operator in the denominator ensures that if the user leaves the PEV connected after the expected plug-off time, the denominator in (4) stays positive. This user convenience function is bounded between minimum $\underline{J} = 0$ and maximum $\overline{J} = 100/\underline{L}$, where $\underline{L}$ is the lowest possible charging rate.

Finally, note that although the user convenience per unit power in (4) is adopted here, any arbitrary user convenience function may be used in its place. The problem formulation does not depend on an specific user convenience function. Moreover, the definition of user convenience has no bearing on the optimality and convergence of the distributed algorithm proposed in the next section.

III. Distributed Charging Strategy

A. Algorithm Description

The goal is to maximize the cumulative user convenience in (1), by selecting a subset of PEVs to charge at each time slot. The rationale of the proposed approach is to collect the user convenience values of all PEVs in a distributed fashion and locally choose the subset of PEVs allowed to charge in order to maximize the cumulative user convenience.

The proposed algorithm involves a two stage procedure. In the first stage, each SA collects and sorts the user convenience values of the PEVs in its area (steps 1-4 of the algorithm). Here, the local power constraints P_k for each SA k are satisfied. In the second stage, a consensus procedure is performed among SAs to allow each SA to collect the user convenience values of all PEVs in the system (step 5 of the algorithm). Then, each SA can locally evaluate a control signal for the PEVs in its area, i.e., a threshold value defining the set of PEVs allowed to charge (steps 6-7 of the algorithm). The global constraint on the available power P is satisfied at this second stage. The proposed algorithm is described by the following steps that are also illustrated in Fig. 2.

1) Computation of User Convenience Value at Each PEV: The i-th PEV of k-th SA locally computes its user convenience, $J_{i,k}$. Then, it transmits $J_{i,k}$, and the rated power $L_{i,k}$, to its SA.

2) Sorting User Convenience Values at Each SA: The SA collects the user convenience values from all PEVs in its area and sorts them in a descending order. For the k-th SA, this ordered set is

$$\mathcal{P}_k = \left\{J_{o_1,k}, J_{o_2,k}, \ldots, J_{o_i,k}, \ldots, J_{o_{N_k},k}\right\} \tag{5}$$

with $o_1, o_2, \ldots, o_{N_k}$ as the indexes of the sorted PEVs in $\mathcal{S}_k$, where

$$J_{o_i,k} \geq J_{o_{i+1},k}, \quad \forall i \in [1, N_k - 1] \tag{6}$$

3) Satisfying Local Power Constraints at Each SA: To satisfy the local power constraints P_k at each SA k, each SA can truncate the ordered set $\mathcal{P}_k$ in (5) such that the total power required by the PEVs in the truncated $\mathcal{P}_k$ is not greater than the available power P_k. Formally, if $\sum_{i=o_1}^{o_{N_k}} L_{i,k} > P_k$, the SA updates the set $\mathcal{P}_k$ as

$$\mathcal{P}_k = \left\{J_{o_1,k}, J_{o_2,k}, \ldots, J_{o_{\tilde{N}_k},k}\right\}, \tag{7}$$

where $\tilde{N}_k$ fulfills the local power limitations, i.e.,

$$\sum_{i=o_1}^{o_{\tilde{N}_k}} L_{i,k} \leq P_k < \sum_{i=o_1}^{o_{\tilde{N}_k+1}} L_{i,k}. \tag{8}$$

4) Building the Histogram of User Convenience Values of the PEVs at Each SA: Since the user convenience function may provide infinite values in the set of real numbers, the collected values in (7) are discretized in arbitrarily small bins (intervals) to obtain a finite set of values. Thus, the range of $J_{i,k}$ values, namely the interval $[\underline{J}, \overline{J}]$, is divided into M bins, such that the m-th bin corresponds to

$$b_m = \left[\underline{J} + (m-1)\Delta, \underline{J} + m\Delta\right] \tag{9}$$

where $\Delta = (\overline{J} - \underline{J})/M$ denotes the bin width. Then, the power requirement of the PEVs in each bin, b_m, is calculated at each SA first. Let $\mathcal{P}_{k,m}$ denote the user convenience values in the set $\mathcal{P}_k$ of the k-th SA which fall within the m-th bin, i.e.,

$$\mathcal{P}_{k,m} = \left\{J_{o_i,k} \in \mathcal{P}_k \text{ and } J_{o_i,k} \in b_m\right\} \tag{10}$$

with power requirement $\rho_{k,m} = \sum_{J_{i,k} \in \mathcal{P}_{k,m}} L_{i,k}$. Thus, it can easily be deduced that

$$\mathcal{P}_k = \bigcup_{m=1}^{M} \mathcal{P}_{k,m}. \tag{11}$$

5) Applying a Consensus Procedure to Find the Total Power Required by PEVs in Each Bin: Since there may be PEVs with $J_{i,k} \in b_m$ connected to different SAs, all SAs have to collaborate to determine the total required power, Γ_m, in each bin b_m. This can be expressed by

$$\Gamma_m = \sum_{k=1}^{K} \rho_{k,m} = K\frac{1}{K}\sum_{k=1}^{K} \rho_{k,m} = K\bar{\Gamma}_m, \quad m \in [1, M]. \tag{12}$$

Thus, the SAs perform a consensus-based procedure to evaluate Γ_m. In detail, the average power requirement of PEVs in each bin, $\bar{\Gamma}_m$, can be computed by running an averaging consensus algorithm [23]. In practice, a certain number of iterations is required to reach consensus, i.e., the consensus procedure stops when each SA knows the total required

This article has been accepted for inclusion in a future issue of this journal. Content is final as presented, with the exception of pagination.

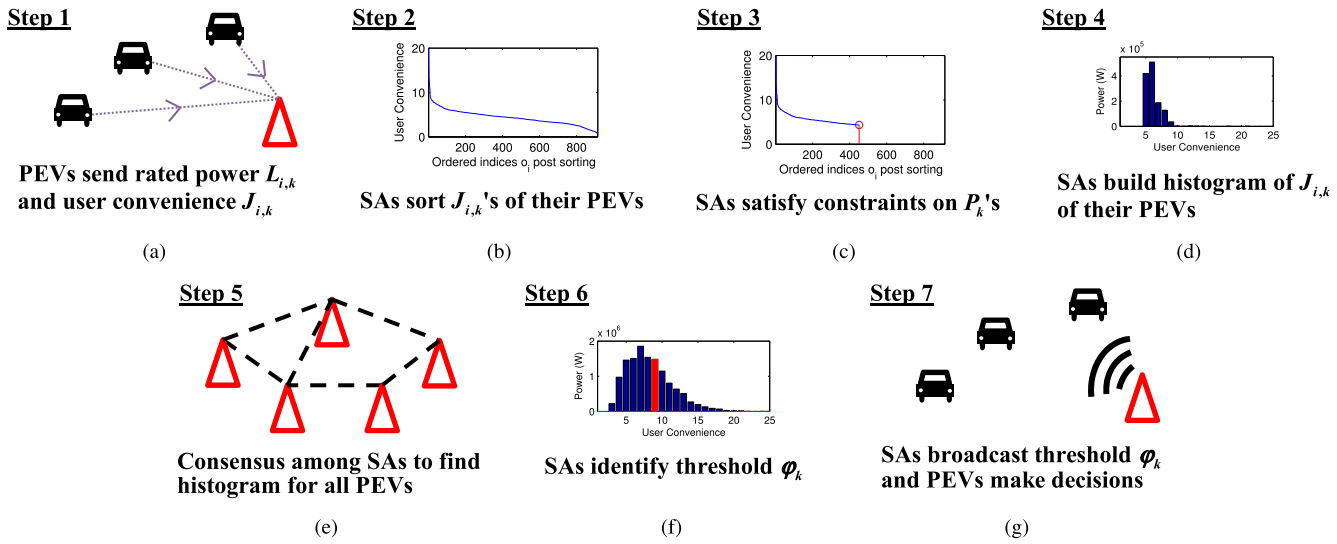

Fig. 2. Summary of the proposed algorithm.

power at bin m, Γ_m. Thus, the following stopping criterion is considered

$$\left\lfloor \hat{\Gamma}^{\tau}_{k,m} K \right\rceil = \left\lfloor \hat{\Gamma}^{\tau}_{k',m} K \right\rceil, \quad \forall k, k' \in \{1, 2, ...K\}, \tag{13}$$

where τ is the iteration number for the consensus procedure and $\hat{\Gamma}^{\tau}_{k,m}$ is the local estimate of Γ_m at the k-th SA after the τ-th iteration, while $\lfloor \cdot \rceil$ denotes the rounding operation. It takes a finite number of iterations to satisfy the stopping criterion in (13) as will be shown later in the case studies.

Finally, the number of SAs, K, is assumed to be known to all the SAs, or it can be computed in a distributed fashion using, e.g., the approach in [24].

6) Finding the Threshold for User Convenience Values to Set the Charging Decision Variables at Each SA: Each SA locally evaluates a threshold value, φ_k, that is a control signal for the PEVs in its area. Only the PEVs with user convenience $J_{i,k}$ greater than the threshold φ_k are allowed to charge in the current time slot. First, each SA computes the cumulative required power,

$$C_m = \sum_{k=m}^{M} \Gamma_k, \tag{14}$$

to charge all PEVs whose user convenience values lie on the $M-m+1$ rightmost bins. Then, assuming the available power P is known, each SA calculates the bin μ where the threshold φ_k lies as follows:

$$\mu = \begin{cases} M, & C_M \geq P \\ m, & C_m \geq P \geq C_{m+1} \\ 1, & P \geq C_1. \end{cases} \tag{15}$$

Thus all PEVs in bins with index greater than μ are allowed to charge, while only some PEVs in bin μ can charge. Since at any SA the exact user convenience values and charging rates of the PEVs from other SAs is not available, each SA can evaluate the power made available to bin μ as

$$\Psi_{k,\mu} = \frac{P - C_{\mu+1}}{\Gamma_\mu} \left(\sum_{J_{i,k} \in \mathcal{P}_{k,\mu}} L_{i,k} \right), \tag{16}$$

i.e., in proportion to the cumulative charging load of the PEVs in the μ-th bin of the SA. Then, the number $i^\star$ of PEVs that can charge from the μ-th bin of the k-th SA is evaluated as

$$\sum_{i=1}^{i^\star} L_{o_i,k} \leq \Psi_{k,\mu} < \sum_{i=1}^{i^\star+1} L_{o_i,k}. \tag{17}$$

Finally, the threshold φ_k, i.e., the control signal for PEVs in its area, is computed as

$$\varphi_k = L_{o_{i^\star},k}. \tag{18}$$

7) Charging Decision at Each PEV: Each SA broadcasts the threshold φ_k to PEVs in its group. Then, each PEV makes a binary charging decision

$$s_{i,k} = \begin{cases} 1, & \text{if } J_{i,k} \geq \varphi_k \\ 0, & \text{otherwise} \end{cases}, \quad \forall k \in \{1, \ldots, K\}, i \in \mathcal{S}_k \tag{19}$$

to decide if the i-th PEV connected to the k-th SA is allowed to charge (when the user convenience $J_{i,k}$ is greater than the threshold φ_k) or not.

B. Optimality Analysis

The cumulative user convenience function J can be rewritten, by exploiting the information about the bin μ where the threshold φ_k lies, as

$$\begin{aligned} J = \sum_{k=1}^{K} \sum_{i=1}^{N_k} J_{i,k} L_{i,k} s_{i,k} &= \sum_{k=1}^{K} \sum_{m=1}^{\mu-1} \sum_{J_{i,k} \in \mathcal{P}_{k,m}} J_{i,k} L_{i,k} s_{i,k} \\ &+ \sum_{k=1}^{K} \sum_{J_{i,k} \in \mathcal{P}_{k,\mu}} J_{i,k} L_{i,k} s_{i,k} \\ &+ \sum_{k=1}^{K} \sum_{m=\mu+1}^{M} \sum_{J_{i,k} \in \mathcal{P}_{k,m}} J_{i,k} L_{i,k} s_{i,k} \end{aligned} \tag{20}$$

Since bins $\{\mu+1, \mu+2, \ldots, M\}$ represent PEVs with higher $J_{i,k}$ that will be charged, and that the PEVs belonging to

This article has been accepted for inclusion in a future issue of this journal. Content is final as presented, with the exception of pagination.

$\{1, 2, \ldots, \mu - 1\}$ cannot be charged, the maximum J in (1) will be

$$\max(J) = \sum_{k=1}^{K} \sum_{m=\mu+1}^{M} \sum_{J_{i,k} \in \mathcal{P}_{k,m}} J_{i,k} L_{i,k} + \max\left(\sum_{k=1}^{K} \sum_{J_{i,k} \in \mathcal{P}_{k,\mu}} J_{i,k} L_{i,k} s_{i,k} \right), \quad (21)$$

where the max in (21) is found such that

$$\sum_{k=1}^{K} \sum_{J_{i,k} \in \mathcal{P}_{k,\mu}} L_{i,k} s_{i,k} \leq P - C_{\mu+1}. \quad (22)$$

Instead, the proposed algorithm due to step (6) can achieve a maximum user convenience, $\max(J^{alg})$, given by

$$\max\left(J^{alg}\right) = \sum_{k=1}^{K} \sum_{m=\mu+1}^{M} \sum_{J_{i,k} \in \mathcal{P}_{k,m}} J_{i,k} L_{i,k} + \sum_{k=1}^{K} \max\left(\sum_{J_{i,k} \in \mathcal{P}_{k,\mu}} J_{i,k} L_{i,k} s_{i,k} \right) \quad (23)$$

which is different from (21) as each SA individually tries to maximize J for its local PEVs connected to it. Each maximization inside the sum in (23) is performed such that

$$\sum_{J_{i,k} \in \mathcal{P}_{k,\mu}} L_{i,k} s_{i,k} \leq \Psi_{k,\mu}. \quad (24)$$

Considering (21) and (23), the following propositions can be derived.

Proposition 1: In a homogeneous scenario (where all PEVs have the same charging rate, i.e., $L_{i,k} = L$, $\forall i, k$), the proposed algorithm maximizes the user convenience in (1) asymptotically as the number of bins increases.

Proof: See Appendix A. ■

Proposition 2: In the general case of a heterogeneous scenario, as the number of bins increases, the proposed algorithm maximizes the user convenience in (1) asymptotically if the μ-th bin has only one PEV. Otherwise, a percentage optimality gap $\epsilon^{\%}$ is defined as

$$\epsilon^{\%} = \left\{ \max\left(\sum_{k=1}^{K} \sum_{J_{i,k} \in \mathcal{P}_{k,\mu}} J_{i,k} L_{i,k} s_{i,k} \right) - \sum_{k=1}^{K} \max\left(\sum_{J_{i,k} \in \mathcal{P}_{k,\mu}} J_{i,k} L_{i,k} s_{i,k} \right) \right\} \Big/ \max(J), \quad (25)$$

where the *max* operators are subject to (22) and (24), respectively.

Proof: See Appendix A. ■

It is worthy to note that the numerator of (25) depends only on the PEV selection from the μ-th bin and, hence, majority of PEVs have no impact on $\epsilon^{\%}$, while the denominator represents all the charging PEVs from a SA. Moreover, the sub-optimality related to the numerator corresponds to just one PEV per SA, i.e., a total of K PEVs in the whole power system. Therefore, as the number of PEVs being charged per SA increases, the optimality gap $\epsilon^{\%}$ goes to zero.

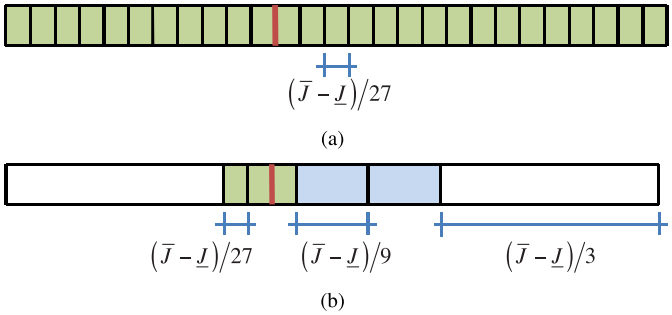

Fig. 3. Example of division of the range $[\underline{J}, \bar{J}]$ with (a) normal procedure and (b) recursive approach. The red line represents the threshold.

C. Recursive Bin Splitting

The proposed algorithm maximizes the objective function in (1) accurately as the number of bins, M, tends to infinity. However, this increases the complexity of the consensus procedure in step (5) of the algorithm. Moreover, such an increment of bins across the entire range $[\underline{J}, \bar{J}]$ is not necessary, since only a small interval of values around the unknown threshold φ_k is beneficial for the proposed algorithm's near optimality (or asymptotically exact in the homogeneous case).

A recursive approach is proposed to trade-off between the algorithm optimality and complexity. The idea is to recursively divide the range of user convenience values into a small number of bins, $\breve{M}$, moving towards the threshold φ_k at each recursion. Therefore, the number of bins around the threshold increases, decreasing the optimality gap, and ensuring asymptotic optimality in the homogeneous case. The sequential processing introduced by the recursive bin splitting may increase the execution time, but the number of computations and communicated data remains the same. However, one can note that this time increment is extremely small (order of seconds) compared to the time slot duration (order of minutes). It will be shown in Appendix B, that the optimal value of $\breve{M}$ for the recursive bin splitting is 3.

Fig. 3 illustrates the idea and the computational advantages of the recursive process. The basic procedure shown in Fig. 3(a) requires the simultaneous consensus on 27 bins. The recursive approach shown in Fig. 3(b) requires the consensus on only 9 bins and a triple execution time. Note that, in both scenarios, the final bin width is the same, i.e., $(\bar{J} - \underline{J})/27$.

IV. Case Studies

A. Tracking Arbitrary Charging Profile

The aim of this section is to show the ability of the proposed algorithm to track any given power profile specified by the grid operator. The algorithm treats the target profile as the total power available for charging, P. Each PEV is assumed to have a 12.5kWh battery with 0% initial SOC. The target SOC is 80% (i.e., a required charge of 10kWh for each PEV). Three possible charging rates are considered: (a) Level 1 charger with 1.4kW, (b) single-phase Level 2 chargers with 3.3kW, and (c) three-phase Level 2 chargers with 6.6kW [25]. Such charger types are considered for 40%, 40% and 20% of the PEVs, respectively. Finally, the value of

This article has been accepted for inclusion in a future issue of this journal. Content is final as presented, with the exception of pagination.

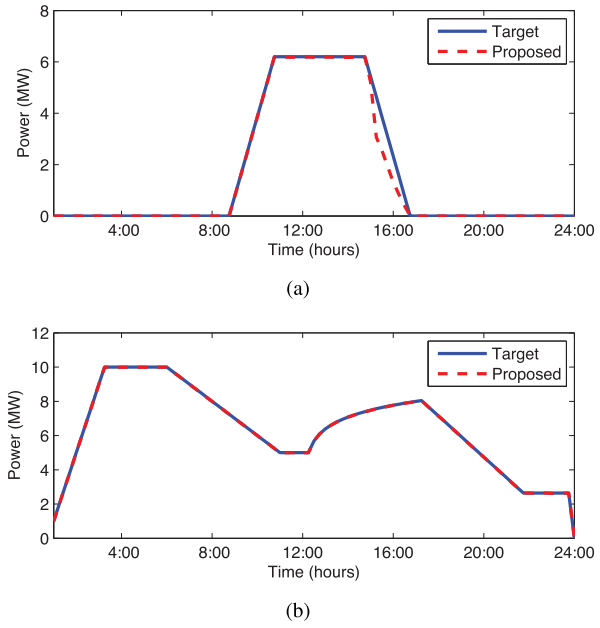

Fig. 4. Tracking examples with two different profiles in (a) and (b).

$\overline{J} = 30/\underline{L}$ is considered, with $\underline{L}$ =1.4kW. A value of $30/\underline{L}$ is used instead of the earlier suggested $100/\underline{L}$ since it has been observed in the simulation that the user convenience never exceeds $30/\underline{L}$.

In Fig. 4(a), up-scaling the simulation setup in [10], 4000 PEVs are assumed to track a target profile with a certain regular shape. A total of 10 sub-aggregators are considered, each with 400 PEVs whose plug-in and plug-off times are uniformly distributed between 9:00-11:00 and 15:00-17:00, respectively. As can be seen from Fig. 4(a), the target profile is closely tracked and the power requirement never exceeds the available power. In the figure, a limited amount of power is not allocated and as a result the power profile with the proposed algorithm dips below the target profile between 16:00 hours and 17:00 hours, this is due to the absence of connected PEVs to charge. Another example with an arbitrary profile to track is illustrated in Fig. 4(b). Here, the profile shape is more variable than in the previous case. A population of 20000 PEVs connected from the first to the last time slot is considered. The profile obtained with the proposed distributed algorithm is the same as the target profile, demonstrating again the effectiveness of the proposed approach.

To compare the solution obtained by the proposed algorithm with the optimal one, the *total optimality gap* (ϵ^{tot}) over a time horizon $[t_0, t_{fin}]$ is defined as a function of the optimality gap $\epsilon^{\%}(t)$ at time slot t in (25)

$$\epsilon^{tot} = \sum_{t=t_0}^{t_{fin}} w(t)\epsilon^{\%}(t), \tag{26}$$

with

$$w(t) = \frac{\min\big(P(t), L^{tot}(t)\big)}{\sum_{t=t_0}^{t_{fin}} \min(P(t), L^{tot}(t))} \tag{27}$$

and

$$L^{tot}(t) = \sum_{k=1}^{K}\sum_{i=1}^{N_k} L_{i,k}. \tag{28}$$

Thus, the total optimality gap is the weighted average of the optimality gap at each time slot of the time horizon, where the weights are proportional to the power required to charge PEVs during the time slot.

For the considered case studies, the total optimality gap is a very small number. In detail, for the target profile in Fig. 4(a), mean and max total optimality gaps are a mere 0.04% and 0.09%, respectively, while for the case given in Fig. 4(b) they are 0.10% and 0.86%, respectively. Thus, the proposed distributed algorithm can effectively track any given profile. Moreover, compared to the existing approaches in [6] and [10] where the power profile of the coordinated charging can potentially go above the target profile to be tracked, the proposed solution guarantees that the coordinated charging profile with our algorithm never goes above the target profile. Such guarantees are necessary since in their absence the algorithms may potentially overload the system resulting into catastrophic outcomes.

B. Obtaining Valley-Filling Profile

The tracking capabilities of the proposed algorithm can be exploited to achieve a valley filling behavior, i.e., to schedule the PEVs during the night hours when the power cost is lower. This case study considers a residential setting with 10000 houses. The daily average load for the houses in the Southern California Edison area [26] is used to generate the base load profile. The set of PEVs includes sedans, compacts, and roadsters with a share of 40%, 40% and 20%, respectively. The batteries of sedans, compacts, and roadsters require 3, 8, and 12 hours of charging with a 3.3kW charger, respectively [25]. Charger types and distribution is the same as considered in the previous case study. Initial SOC is considered to be a Gaussian distributed random variable with mean at 0.5 and variance of 0.1 [8]. Plug-in and plug-off times are Gaussian distributed random variables with means at 5 PM and 7 AM (the next day), respectively, while their variances are considered to be 2 hours and 1 hour, respectively [8]. The target SOC is 80%. The average number of PEVs per household is 1.86 based on the National Household Travel Survey [27].

A total of 10 sub-aggregators with 15%, 14%, 13%, 12%, 10%, 10%, 8%, 7%, 6%, 5% of the PEVs, respectively, are considered in this case study. The power constraints are in line with [6]. The constraints on total available power, P, is set as the maximum value of the base load curve. In detail, the local power constraints at each sub-aggregator, P_k, are set to be 25% larger than the mean power requirement across all sub-aggregators. On average, 10% of PEVs are connected to a sub-aggregator and, hence, P_k is the power required to charge 12.5% of PEVs.

In Fig. 5(a), the proposed algorithm is shown to allocate the PEVs load to non-peak periods, unlike the uncoordinated PEV charging that increases the peak load. This case study considers the scenario with 20% PEV penetration level and

This article has been accepted for inclusion in a future issue of this journal. Content is final as presented, with the exception of pagination.

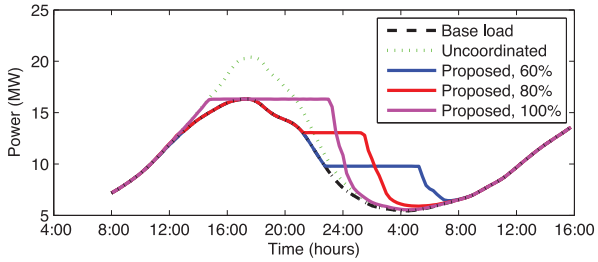

(a)

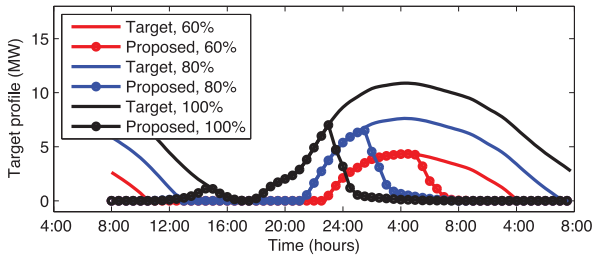

(b)

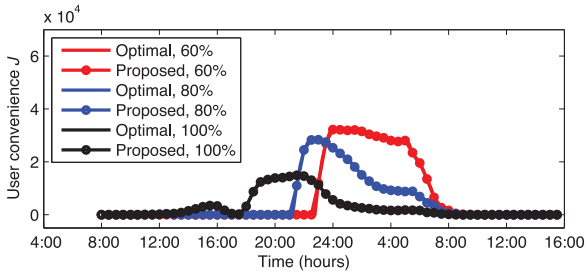

(c)

Fig. 5. Example of obtaining a valley-filling behavior: (a) aggregated load profile including PEVs, (b) profile to track for PEV charging only, and (c) cumulative user convenience values.

three different target profiles for the proposed algorithm. The three target profiles are considered to be 60%, 80%, and 100% of the peak base-load profile, respectively. As can be inferred from Fig. 5(a), the proposed algorithm closely follows the target profiles in all three cases. Indeed, in a practical scenario, the available power for PEV charging can be defined considering the generation capacity of the utility in conjunction with forecasts of base and PEV loads. Fig. 5(b) shows the three different target profiles to track for the proposed algorithm. The charging profile never exceeds the available power and closely follows the target profile. Thus, the proposed algorithm can be effectively exploited to obtain a valley filling profile. Finally, the cumulative user convenience value is illustrated in Fig. 5(c) for both the optimal case and the proposed algorithm, under different target profiles. These curves nearly overlap at all time instants. Thus, the proposed algorithm can achieve near-optimality in a heterogeneous setup, as also reported in Proposition 2.

C. Numerical Performance

Table I and II present statistical information about the algorithm performance at 20%, 50%, and 100% PEV penetration levels with the target SOC of 80% and 100%, respectively.

TABLE I
COMPARISON OF SOC AT DIFFERENT PENETRATION LEVELS WITH TARGET SOC AS 80%

Penetration level	$Pr70$	$Pr75$	$Pr80$	$\overline{SOC}$	ϵ^{tot}
20%	99.92	99.75	99.44	79.98	0.22
50%	99.91	99.74	98.40	79.97	0.14
100%	93.68	81.91	52.45	77.44	0.10

TABLE II
COMPARISON OF SOC AT DIFFERENT PENETRATION LEVELS WITH TARGET SOC AS 100%

Penetration level	$Pr70$	$Pr80$	$Pr90$	$Pr100$	$\overline{SOC}$	ϵ^{tot}
20%	99.90	99.42	97.50	93.86	99.39	0.14
50%	99.87	99.01	94.06	74.99	98.20	0.08
100%	74.98	58.74	26.05	4.44	79.28	0.07

TABLE III
COMPARISON OF APPROXIMATION ERROR WITH DIFFERENT NUMBER OF RECURSIVE BIN SPLITTING ITERATIONS

Bin splitting iterations	**Actual bin number**	**Effective bin number**	**Mean** ϵ^{tot} (%)	**Max** ϵ^{tot} (%)
1	3	3	8.37	24.67
2	6	9	8.37	24.67
3	9	27	8.28	24.58
4	12	81	3.02	12.38
5	15	243	0.32	2.26
6	18	729	0.10	0.59

A target profile such that the aggregated profile does not exceed 100% of the peak of the base load profile has been considered. *PrX* represents percentage of PEVs with SOC greater than *X*% at the plug-off time, while $\overline{SOC}$ is the mean of the final SOC. The values obtained have been found over 100 runs of the algorithm. It is possible to note that the total optimality gap is about 0.1-0.2%, irrespective of the number of PEVs to charge. In the 20% penetration case, there are 3720 PEVs to be charged and almost all of them reach the target SOC of 80%. Similar results are reported for the 50% penetration case with 9300 PEVs. Even for the extreme case of 100% penetration, more than 90% of the PEVs achieve 70% SOC, with an average SOC of 77%, and with a negligible optimality gap of 0.10%. Naturally, not all PEVs achieve the target SOC due to the limited available power. For the 100% target SOC case with 20% and 50% PEV penetration levels, almost all PEVs reach the target SOC. Finally, it is worthy to note that the total optimality gap is even smaller for 100% target SOC compared to the previous case with 80% target SOC.

Table III shows that the recursive bin splitting reduces the difference between the optimal solution and the one achieved by the proposed algorithm, while linearly increasing the number of actual bins. Indeed, for a single splitting operation, the mean and maximum total optimality gaps are 8.37% and 24.67%, respectively. Instead, with 6 splitting operations, the number of actual bins is increased only to 18, while the mean and maximum total optimality gaps are reduced to the very small values of 0.10% and 0.59%, respectively.

D. Algorithm Complexity and Scalability

This section investigates the algorithm complexity by comparison with a distributed algorithm based on the well-known

This article has been accepted for inclusion in a future issue of this journal. Content is final as presented, with the exception of pagination.

TABLE IV
COMPARISON OF PROPOSED ALGORITHM AND ADMM-BASED ALGORITHM IN [6]

Communications	Proposed algorithm	
	Transmission	Reception
At PEV	2 to SA	1 from SA
At SA	$M\|\mathcal{N}\|I_1$ to SAs 1 broadcast to PEVs	$M\|\mathcal{N}\|I_1$ from SAs $2N_k$ from PEVs
At AGG	none	none

Communications	ADMM-based algorithm in [6]	
	Transmission	Reception
At PEV	I_2 to SA	$2I_2$ from SA
At SA	I_2 to AGG $2I_2$ broadcast to PEVs	$2I_2$ from AGG $N_k I_2$ from PEVs
At AGG	$2KI_2$ to SAs	KI_2 from SAs

ADMM method [6]. Considering the distributed nature of the algorithms, it is worthy to note that the method in [6] requires a central aggregator in addition to the SAs, and it cannot guarantee the fulfillment of the power constraints (which are reported to be violated in 5% cases even after 60 iterations [6]). A summary of the required communications for both the proposed algorithm and [6] is summarized in Table IV, considering PEVs, SAs, and the central aggregator (AGG) for [6], where M is the number of bin splitting operations and I_1 is the number of iterations to reach consensus for the proposed algorithm, while I_2 is the number of ADMM iterations in [6].

Let us consider a case study with 20000 PEVs, equally distributed among 10 SAs, where each SA can communicate on average with a number of neighbor SAs, $\mathcal{N}$, equal to $|\mathcal{N}| = 4.8$. The proposed algorithm requires six bin splitting operations (i.e., $M = 18$) and 70 iterations ($I_1 = 70$) to reach a consensus on (12), while the work in [6] requires $I_2 = 60$ ADMM iterations. Note that the number of consensus iterations, I_1, for the proposed algorithm has been chosen equal to 70 since a campaign of experiments performed with random connections among the SAs has reported that 66 iterations are required on average. For every charging interval, at each SA, the proposed algorithm exchanges a total of 12×10^3 units of data with its neighbors, and receives 4×10^3 units of data from the PEVs, and broadcasts just one unit of data to the PEVs. The ADMM-based algorithm exchanges only 180 units of data with the central aggregator, but receives 1.2×10^5 units of data from the PEVs, and has to broadcast 120 units of data to the PEVs. Thus, one can note that the total amount of data required for both transmission and reception is about one order of magnitude less with the proposed algorithm compared to the ADMM-based algorithm in [6].

Finally, one can note that the communication overhead for the proposed approach is increased by only one transmission per PEV for every new PEV added. Indeed, the PEV parameters have to be sent to the SA only once during each time interval. On the other hand, the algorithm in [6] requires a communication overhead of the order of the number of ADMM iterations, I_2. Considering a typical value of $I_2 = 60$ [6], it is straightforward to note that the proposed approach exhibits a better scalability property compared to the literature. Thus, the order of the transmission data and the improved scalability shows the efficiency of the proposed distributed approach.

V. CONCLUSION

A distributed algorithm for PEV coordinated charging is proposed to maximize the user convenience under the power constraints imposed by the power utility. It can track any given power profile provided by the power utility, while maximizing the user satisfaction in terms of state of charge and charging time. The heterogeneity in the charging rates has been included to incorporate PEVs charging process at residence, parking lots, or charging stations, into a unified coordination framework. Moreover, discrete charging rates have been considered to accommodate for the limitation imposed by the charger technologies. The algorithm is implemented in a distributed fashion by exploiting consensus algorithms for inter-sub-aggregator communications, thus it is easily scalable and tolerant to network faults. The effectiveness of the algorithm has been demonstrated in realistic scenarios, with a heterogeneous PEVs population, under different penetration levels. As a particular case of the tracking feature, the proposed distributed algorithm has also been shown to be effective to track valley-filling profiles. Finally, future work will investigate alternative user convenience functions capturing other potential aspects of interest, e.g., economical issues.

APPENDIX A
OPTIMALITY ANALYSIS OF THE ALGORITHM

A. Proof of Proposition 1

Let us consider the asymptotic behavior, i.e., $M \to \infty$, in the simplified case of a homogeneous scenario. Each bin b_m has bin-width $\Delta \to 0$, and every user convenience value in $[\underline{J}, \overline{J}]$ is represented by a distinct bin. Considering (21) and (23), one can note that the optimality depends only on the sub-selection in μ-th bin. Let η_μ be the PEV number in μ-th bin, then the following two cases may be verified.

1) $\eta_\mu = 1$: The only PEV in bin μ, say $\tilde{i}$, is assumed to be connected to SA $\tilde{k}$. Then, from (21), it follows

$$\max\left(\sum_{k=1}^{K}\sum_{J_{i,k}\in\mathcal{P}_{k,\mu}} J_{i,k}L_{i,k}s_{i,k}\right) = J_{\tilde{i},\tilde{k}}L_{\tilde{i},\tilde{k}} \tag{29}$$

and, from (23), it follows

$$\sum_{k=1}^{K}\max\left(\sum_{J_{i,k}\in\mathcal{P}_{k,\mu}} J_{i,k}L_{i,k}s_{i,k}\right) = J_{\tilde{i},\tilde{k}}L_{\tilde{i},\tilde{k}}, \tag{30}$$

under the constraints in (22) and (24), respectively. Thus, the proposed algorithm achieves the result in (30) which is equal to the optimal one in (29).

2) $\eta_\mu > 1$: The μ-th bin has more than one PEV, thus sub-selection is required. However, since all PEVs in μ-th bin have the same user convenience values, any of them can be selected without affecting the result. Thus, the proposed algorithm is also optimal in this case.

B. Proof of Proposition 2

Let us consider the asymptotic behavior in the general case of heterogeneous scenario. Similar to the previous proof, two cases are considered.

This article has been accepted for inclusion in a future issue of this journal. Content is final as presented, with the exception of pagination.

1) $\eta_\mu = 1$: The argument presented in Appendix A-A1 is repeated, and the optimal solution is achieved by the proposed algorithm.

2) $\eta_\mu > 1$: Optimality gap ϵ in (25) directly follows from (21) and (23).

APPENDIX B
OPTIMAL NUMBER OF BINS

We demonstrate that the optimal number of bins $\breve{M}$ for the recursive bin splitting operation is 3. Let x and y denote the number of recursions and bins, respectively. If the consensus averaging is done for a maximum of M bins, it is required to maximize $y = (\breve{M})^x$ under the constraint that $x \cdot \breve{M} = M$. Then,

$$ln(y) = \frac{M}{\breve{M}} ln\big(\breve{M}\big) \tag{31}$$

Differentiating both sides yields

$$\frac{1}{y}\frac{dy}{d\breve{M}} = -\frac{M}{\breve{M}^2} ln\big(\breve{M}\big) + \frac{M}{\breve{M}^2} \tag{32}$$

$$\frac{dy}{d\breve{M}} = \frac{M}{\breve{M}^2}\big[1 - ln\big(\breve{M}\big)\big]\breve{M}^{M/\breve{M}} \tag{33}$$

Setting $dy/d\breve{M} = 0$ and finding the maximum of the cost function leads to

$$\frac{M}{\breve{M}^2}[1 - ln(x)]\breve{M}^{M/\breve{M}} = 0. \tag{34}$$

Considering finite values of $\breve{M}$ yields

$$1 - ln\big(\breve{M}\big) = 0, \text{and } \breve{M} = e. \tag{35}$$

Since $\breve{M}$ should be an integer we set the number of bins for the recursive bin splitting operation is 3, i.e., the closest integer to e.

REFERENCES

[1] P. Denholm and W. Short, "An evaluation of utility system impacts and benefits of optimally dispatched plug-in hybrid electric vehicles," Nat. Renew. Energy Lab., Golden, CO, USA, Tech. Rep. NREL/TP-620-40293, 2006.

[2] S. Shafiee, M. Fotuhi-Firuzabad, and M. Rastegar, "Investigating the impacts of plug-in hybrid electric vehicles on power distribution systems," *IEEE Trans. Smart Grid*, vol. 4, no. 3, pp. 1351–1360, Sep. 2013.

[3] L. P. Fernández, T. G. S. Román, R. Cossent, C. M. Domingo, and P. Frías, "Assessment of the impact of plug-in electric vehicles on distribution networks," *IEEE Trans. Power Syst.*, vol. 26, no. 1, pp. 206–213, Feb. 2011.

[4] Q. Gong, S. Midlam-Mohler, V. Marano, and G. Rizzoni, "Study of PEV charging on residential distribution transformer life," *IEEE Trans. Smart Grid*, vol. 3, no. 1, pp. 404–412, Mar. 2012.

[5] E. Veldman and R. A. Verzijlbergh, "Distribution grid impacts of smart electric vehicle charging from different perspectives," *IEEE Trans. Power Syst.*, vol. 6, no. 1, pp. 333–342, Jan. 2015.

[6] C.-K. Wen, J.-C. Chen, J.-H. Teng, and P. Ting, "Decentralized plug-in electric vehicle charging selection algorithm in power systems," *IEEE Trans. Smart Grid*, vol. 3, no. 4, pp. 1779–1789, Dec. 2012.

[7] W. Su and M.-Y. Chow, "Performance evaluation of an EDA-based large-scale plug-in hybrid electric vehicle charging algorithm," *IEEE Trans. Smart Grid*, vol. 3, no. 1, pp. 308–315, Mar. 2012.

[8] G. Binetti, A. Davoudi, D. Naso, B. Turchiano, and F. L. Lewis, "Scalable real-time electric vehicles charging with discrete charging rates," *IEEE Trans. Smart Grid*, vol. 6, no. 5, pp. 2211–2220, Sep. 2015.

[9] G. Wang, J. Zhao, F. Wen, Y. Xue, and G. Ledwich, "Dispatch strategy of PHEVs to mitigate selected patterns of seasonally varying outputs from renewable generation," *IEEE Trans. Smart Grid*, vol. 6, no. 2, pp. 627–639, Mar. 2015.

[10] L. Gan, U. Topcu, and S. Low, "Optimal decentralized protocol for electric vehicle charging," *IEEE Trans. Power Syst.*, vol. 28, no. 2, pp. 940–951, May 2013.

[11] N. Chen, C. W. Tan, and T. Q. S. Quek, "Electric vehicle charging in smart grid: Optimality and valley-filling algorithms," *IEEE J. Emerg. Sel. Topics Power Electron.*, vol. 8, no. 6, pp. 1073–1083, Dec. 2014.

[12] A. Di Giorgio, F. Liberati, and S. Canale, "Electric vehicles charging control in a smart grid: A model predictive control approach," *Control Eng. Pract.*, vol. 22, pp. 147–162, Jan. 2014.

[13] Z. Li, Q. Guo, H. Sun, and S. Xin, "A decentralized optimization method to track electric vehicle aggregator's optimal charging plan," in *Proc. IEEE PES Gen. Meeting Conf. Expo.*, 2014, pp. 1–5.

[14] C. Ahn, C.-T. Li, and H. Peng, "Optimal decentralized charging control algorithm for electrified vehicles connected to smart grid," *J. Power Sources*, vol. 196, no. 23, pp. 10369–10379, Dec. 2011.

[15] T. M. Bandhauer, S. Garimella, and T. F. Fuller, "A critical review of thermal issues in lithium-ion batteries," *J. Electrochem. Soc.*, vol. 158, no. 3, pp. R1–R25, 2011.

[16] L. Gan, U. Topcu, and S. H. Low, "Stochastic distributed protocol for electric vehicle charging with discrete charging rate," in *Proc. IEEE Power Energy Soc. Gen. Meeting*, San Diego, CA, USA, 2012, pp. 1–8.

[17] S. Han, S. Han, and K. Sezaki, "Development of an optimal vehicle-to-grid aggregator for frequency regulation," *IEEE Trans. Smart Grid*, vol. 1, no. 1, pp. 65–72, Jun. 2010.

[18] Y. He, B. Venkatesh, and L. Guan, "Optimal scheduling for charging and discharging of electric vehicles," *IEEE Trans. Smart Grid*, vol. 3, no. 3, pp. 1095–1105, Sep. 2012.

[19] D. Wu, D. C. Aliprantis, and L. Ying, "Load scheduling and dispatch for aggregators of plug-in electric vehicles," *IEEE Trans. Smart Grid*, vol. 3, no. 1, pp. 368–376, Mar. 2012.

[20] V. Robu *et al.*, "An online mechanism for multi-speed electric vehicle charging," in *Auctions, Market Mechanisms, and Their Applications*. Berlin, Germany: Springer-Verlag, 2012, pp. 100–112.

[21] O. Ardakanian, S. Keshav, and C. Rosenberg, "Real-time distributed control for smart electric vehicle chargers: From a static to a dynamic study," *IEEE Trans. Smart Grid*, vol. 5, no. 5, pp. 2295–2305, Sep. 2014.

[22] S. Shao, M. Pipattanasomporn, and S. Rahman, "Demand response as a load shaping tool in an intelligent grid with electric vehicles," *IEEE Trans. Smart Grid*, vol. 2, no. 4, pp. 624–631, Dec. 2011.

[23] L. Xiao and S. Boyd, "Fast linear iterations for distributed averaging," in *Proc. 42nd IEEE Conf. Decis. Control*, Maui, HI, USA, 2003, pp. 4997–5002.

[24] G. Binetti, A. Davoudi, F. L. Lewis, D. Naso, and B. Turchiano, "Distributed consensus-based economic dispatch with transmission losses," *IEEE Trans. Power Syst.*, vol. 29, no. 4, pp. 1711–1720, Jul. 2014.

[25] A. Ipakchi and F. Albuyeh, "Grid of the future," *IEEE Power Energy Mag.*, vol. 7, no. 2, pp. 52–62, Mar./Apr. 2009.

[26] (Jul. 1, 2015). *South California Edison (SCE) Website*. [Online]. Available: http://www.sce.com

[27] U.S. Department of Transportation. (Jul. 1, 2015). *2009 National Household Travel Survey*. [Online]. Available: http://nhts.ornl.gov/2009/pub/stt.pdf

Akshay Malhotra received the B.Eng. degree from the PES Institute of Technology, Bengaluru, India, in 2011. He is currently pursuing the Master's degree in science with the Department of Electrical Engineering, University of Texas at Arlington, TX, USA. His research focuses on distributed signal processing and electric vehicle charging strategies.

This article has been accepted for inclusion in a future issue of this journal. Content is final as presented, with the exception of pagination.

Giulio Binetti (S'11–M'15) received the Ph.D. degree in electrical and information engineering from the Polytechnic of Bari, Bari, Italy, in 2014. He was a Research Scholar and a Research Assistant with the University of Texas, Arlington, TX, USA. He is currently a Postdoctoral Research Fellow with the Polytechnic of Bari. His current research interests include distributed algorithms, auction theory, smart grid, and electric vehicles.

Ali Davoudi (S'04–M'08–SM'15) received the Ph.D. degree in electrical and computer engineering from the University of Illinois, Urbana, IL, USA, in 2010. He is currently an Assistant Professor with the University of Texas, Arlington, TX, USA. His research interests include control of power electronics and finite-inertia power systems. He is an Associate Editor of the IEEE TRANSACTIONS ON ENERGY CONVERSION, the IEEE TRANSACTIONS ON INDUSTRY APPLICATION, and the IEEE TRANSACTIONS ON TRANSPORTATION ELECTRIFICATION.

Ioannis D. Schizas (M'12) received the Ph.D. degree in electrical and computer engineering from the University of Minnesota, Minneapolis, in 2011. He has been an Assistant Professor with the Electrical Engineering Department, University of Texas, Arlington, TX. His research interests lie in the areas of statistical signal processing, learning techniques, and tracking.